

Accepted Manuscript

Synthetic sulfoglycolipids targeting the serine-threonine protein kinase Akt

Barbara Costa, Milind Dangate, Maria Vetro, Giulia Donvito, Luca Gabrielli, Loredana Amigoni, Giuliana Cassinelli, Cinzia Lanzi, Michela Ceriani, Luca De Gioia, Giulia Filippi, Laura Cipolla, Nadia Zaffaroni, Paola Perego, Diego Colombo

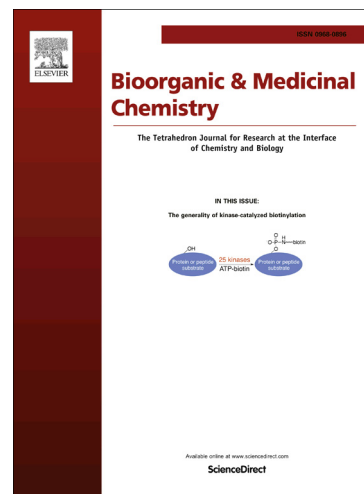
PII: S0968-0896(16)30355-8
DOI: <http://dx.doi.org/10.1016/j.bmc.2016.05.031>
Reference: BMC 13015

To appear in: *Bioorganic & Medicinal Chemistry*

Received Date: 14 January 2016
Revised Date: 22 April 2016
Accepted Date: 17 May 2016

Please cite this article as: Costa, B., Dangate, M., Vetro, M., Donvito, G., Gabrielli, L., Amigoni, L., Cassinelli, G., Lanzi, C., Ceriani, M., Gioia, L.D., Filippi, G., Cipolla, L., Zaffaroni, N., Perego, P., Colombo, D., Synthetic sulfoglycolipids targeting the serine-threonine protein kinase Akt, *Bioorganic & Medicinal Chemistry* (2016), doi: <http://dx.doi.org/10.1016/j.bmc.2016.05.031>

This is a PDF file of an unedited manuscript that has been accepted for publication. As a service to our customers we are providing this early version of the manuscript. The manuscript will undergo copyediting, typesetting, and review of the resulting proof before it is published in its final form. Please note that during the production process errors may be discovered which could affect the content, and all legal disclaimers that apply to the journal pertain.



Synthetic sulfoglycolipids targeting the serine-threonine protein kinase Akt

Barbara Costa,^[a] Milind Dangate,^{[b][†]} Maria Vetro,^{[b][×]} Giulia Donvito,^[a] Luca Gabrielli,^[a] Loredana Amigoni,^[a] Giuliana Cassinelli,^[c] Cinzia Lanzi,^[c] Michela Ceriani,^[a] Luca De Gioia,^[a] Giulia Filippi,^[a] Laura Cipolla,^[a] Nadia Zaffaroni,^[c] Paola Perego,^{[c]*} and Diego Colombo^[b]

^[a] Department of Biotechnology and Biosciences, University of Milano-Bicocca, P.za della Scienza 2, 20126 Milan, Italy

^[b] Department of Medical Biotechnology and Translational Medicine, University of Milano, Via Saldini 50, 20133 Milan, Italy

^[c] Molecular Pharmacology Unit, Fondazione IRCCS Istituto Nazionale dei Tumori, Via Amadeo 42, 20133 Milan, Italy

^[†] Present address: Amrita Vishwa Vidyapeetham, School of Arts and Sciences, Department of Chemistry, Amritapuri, Clappana P.O., Kollam – 690 525, Kerala, India

^[×] Present address: Center for Synthesis and Chemical Biology, University College Dublin, Belfield, Dublin 4, Ireland

*Corresponding author: Paola Perego, paola.perego@istitutotumori.mi.it

ABBREVIATIONS

phosphoinositide 3-kinase, PI3K; PH, pleckstrin homology; 4IP, inositol-(1,3,4,5)-tetrakisphosphate; PI3P, 3-phosphorylated phosphatidylinositol; PTC, papillary thyroid carcinoma; SQAG, sulfoquinovosylacylglycerols.

Abstract

The serine-threonine protein kinase Akt, also known as protein kinase B, is a key component of the phosphoinositide 3-kinase (PI3K)-Akt-mTOR axis. Deregulated activation of this pathway is frequent in human tumors and Akt-dependent signaling appears to be critical in cell survival. PI3K activation generates 3-phosphorylated phosphatidylinositols that bind Akt pleckstrin homology (PH) domain. The blockage of Akt PH domain/phosphoinositides interaction represents a promising approach to interfere with the oncogenic potential of over-activated Akt. In the present study, phosphatidyl inositol mimics based on a β -glucoside scaffold have been synthesized as Akt inhibitors. The compounds possessed one or two lipophilic moieties of different length at the anomeric position of glucose, and an acidic or basic group at C-6. Docking studies, ELISA Akt inhibition assays, and cellular assays on different cell models highlighted 1-*O*-octadecanoyl-2-*O*- β -D-sulfoquinovopyranosyl-*sn*-glycerol as the best Akt inhibitor among the synthesized compounds, which could be considered as a lead for further optimization in the design of Akt inhibitors.

KEYWORDS: sulfoquinovose, phosphatidyl inositol analogues, inhibitors, Akt, cancer

1. Introduction

Kinase inhibitors have attracted considerable attention over the past decade as anti-cancer agents and several kinase targeting agents have reached the clinical setting [1-4]. Kinases, through the phosphorylation of specific protein and non-protein targets, are enzymes involved in the regulation of many crucial cellular processes such as proliferation, differentiation and apoptosis [5-7]. Among them, the serine/threonine protein kinase Akt, also known as protein kinase B, plays a key role as a component of the phosphoinositide 3-kinase (PI3K)-Akt-mTOR axis, which is implicated in aberrant tumor cell signaling [8-9]. Deregulated activation of this pathway is a common event in human tumors and Akt-dependent signaling appears to be critical in cell survival [8]. Thus, inhibitors that target PI3K and its downstream effectors, including Akt, are relevant for cancer therapy [10-14]. PI3K activation generates 3-phosphorylated phosphatidylinositols (PI3Ps), that bind Akt pleckstrin homology (PH) domain [15-17]. The interaction between the PH domain and phosphoinositide induces a conformational change of Akt, allowing the kinase full activation by two phosphorylations (Thr308 and Ser473) [18]. Thus, the blockage of Akt PH domain/phosphoinositide interaction represents a promising approach to interfere with the oncogenic potential of overactivated Akt.

Several inhibitors targeting the PH domain have been proposed in the last years, including phosphoinositide analogues, alkylphospholipids and inositol phosphates [11]. Though synthetic carbohydrate-based mimics of inositols have already been reported [19], a few examples on the use of glucose as scaffold for the design of Akt inhibitors have been described [20, 21]. Here, we present the synthesis and the biological activity of new sulphoglycolipids structurally related to the natural sulfoquinovosylacylglycerols (SQAG, **1**, Figure 1), a family of natural compounds associated with photosynthetic organisms in which sulfoquinovose (6-deoxy-6-sulfolucose) is α -linked to the *sn*-3 position of an acylglycerol [22, 23].

SQAG, which inspired this work, have been already considered as promising compounds in different therapeutic areas, including anti-cancer therapy. In fact, members of this class of compounds have been described as inhibitors of HIV-reverse transcriptase or of the mammalian DNA polymerase. Moreover, inhibitory activity on cancer cell proliferation as well as apoptosis induction and *in vivo* antitumor and anti-angiogenic effects have been reported [24]. Nevertheless, to our knowledge their Akt inhibitory activity in relation to inhibition of cancer cell proliferation has not been reported. Differently from SQAG, compounds **2a-c** and **3a-c** (Figure 1) are based on a 2-*O*- β -D-glucopyranosyl-*sn*-glycerol scaffold, thus representing a novel class of potential Akt inhibitors acting as phosphoinositide mimics targeting the Akt PH domain. The structure of phosphatidylinositol-3-phosphate, a natural ligand of Akt PH domain, (PI3P, Figure 1) as produced by PI3K, can resemble a suitably modified D-glucose scaffold, where specific functional groups can be introduced.

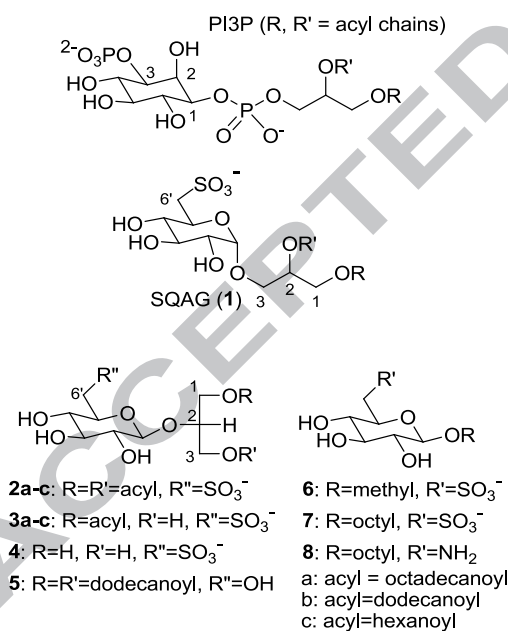


Figure 1

Thus, we synthesized a series of D-glucopyranose compounds (Figure 1) endowed with the following key features needed for the interaction with the PH domain: i) an anionic group mimicking the phosphate group in position 3 of the inositol (position 6 of the sugar), that should

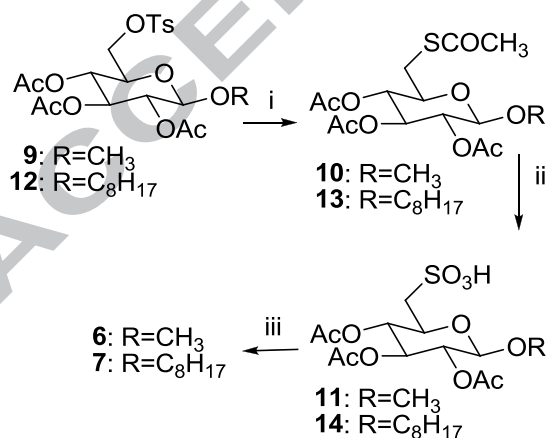
be able to form a salt bridge with a key arginine residue [20]; ii) a β -configured substituent at the anomeric carbon of D-glucopyranose (position 1 of inositol) possessing a hydrogen-donor heteroatom and a lipophilic group mimicking the diacyl glycerol moiety of phosphoinositides. The long lipophilic acyl chains of the natural phosphatidylinositol-3-phosphate substrate can be substituted by shorter hydrophobic groups, since the long fatty acid chain is not needed for enzyme recognition, but only for membrane anchoring [16]. In addition, the lack of the hydroxyl group in position 2 of the inositol ring, substituted by the pyranosidic oxygen of the sugar, does not alter enzyme recognition.

2. Results and Discussion

2.1 Chemistry. Synthesis of inhibitors 2-8

Recently, as part of an exploratory study evaluating the potential anti-tumor-promoting activities of glycoacylglycerolipids, we synthesized [25, 26] a series of analogues of SQAG in which sulfoquinovose is β -linked to the 2 position of an acylglycerol (diacylglycerol **2a-c** or monoacylglycerol **3a-c**). In the D-glucose-based skeleton, the presence of the stable (non-hydrolysable) anionic sulfonate group at the 6 position and the β -acylglycerol aglycone directly linked to the sugar (lacking the phosphate bridge), convert such compounds into a sort of hybrid between PI3P and the SQAG **1**. For these reasons, we decided to evaluate the Akt inhibitory activity of compounds **2a-c** and **3a-c**. In addition, to obtain further SAR data, we prepared and tested as potential Akt inhibitors the fully deacylated sulfoquinovosyl-2-*O*- β -D-glycerol **4**, the glucoglycerolipid **5** lacking the characteristic sulfonate group of sulfoquinovosides, the methyl and octyl- β -D-sulfoquinovosides **6** and **7** lacking the glycerol moiety and the derivative **8**

carrying a cationic (instead of an anionic) amino group. 1,3-Di-*O*-acyl-2-*O*- β -D-sulfoquinovopyranosyl-*sn*-glycerols **2a-c** [25], 1,3-di-*O*-dodecanoyl-2-*O*- β -D-glucopyranosyl-*sn*-glycerol **5** [25], 1-*O*-acyl-2-*O*- β -D-sulfoquinovopyranosyl-*sn*-glycerols **3a-c** [26] and 6-amino-6-deoxy-glucoside **8** [27] were prepared as previously reported. The fully deacylated 2-*O*- β -D-sulfoquinovopyranosyl-*sn*-glycerol **4** was obtained by Zemplén reaction from a small amount of compound **3a**. Methyl β -D-sulfoquinovopyranoside **6** [28] was prepared by converting the known methyl 2,3,4-tri-*O*-acetyl-6-*O*-tosyl- β -D-glucopyranoside (**9**) [29] into the corresponding 6-thioacetyl glucoside (**10**) by potassium thioacetate treatment in DMF, following Oxone[®] oxidation to the corresponding sulfonate **11** and final acetyl groups removal by Zemplén reaction (Scheme 1). A similar synthetic scheme was used to obtain the octyl sulfoquinovoside **7**. To this end octyl 2,3,4-tri-*O*-acetyl-6-*O*-tosyl- β -D-glucopyranoside **12**, obtained one pot from commercial octyl β -D-glucopyranoside by tosyl chloride treatment in pyridine at low temperature followed by direct acetylation with acetic anhydride, was converted into the corresponding thioacetate **13**, oxidized to the triacetylsulfonate **14** and deacetylated to yield the desired octyl β -D-sulfoquinovopyranoside **7** (Scheme 1).



Scheme 1 i: CH₃COSK, DMF; ii: OXONE[®], CH₃COOH; iii: CH₃ONa, CH₃OH

2.2 Evaluation of Akt inhibition in cell-free assay (ELISA)

The synthesized derivatives **2-8**, with the exception of compound **2a** that was not soluble in DMSO, were assayed *in vitro* for inhibitory activity against Akt, using a cell-free assay, at fixed concentration of 100 μM (Figure 2). The data showed that, **2b** and **3a** were the most active derivatives, possessing long or medium acyl chains and the anionic $-\text{SO}_3^-$ group at carbon 6 of the sugar moiety. Compounds **4** and **8**, the first missing the acyl chains, the second with a positively-chargeable amino group in place of the sulphonyl group at C-6 were among the least active ones, in agreement with the docking studies (see below). These data suggest that a lipophilic moiety mimicking the diacylglycerol group of PI3P is needed for a better interaction with the kinase (polar glycerol OH groups in **4** are detrimental for activity), whereas cationic groups could not be accepted by the enzymatic pocket, because of repulsive ionic interaction between the ammonium group and the Arg side chain [20]. Furthermore, both the acyl and anionic groups are needed for high activity, the lack of one of them lowering the activity below 13% inhibition (Figure 2). Compound **5**, endowed with medium length acyl chains (dodecanoyl groups), but possessing the $-\text{OH}$ instead of the anionic group at C-6 displayed a tenfold lower activity than the corresponding sulphonate **2b**, thereby confirming that the anionic group is relevant for the activity, as already observed for a glucuronosylglycerol series [30]. In addition, the length of the acyl chain appears to influence the potency of the sulphonate series **2** and **3**. In fact, the longer the chain, the higher the activity, whereas the number of acyl chains seems to be less relevant (Figure 2).

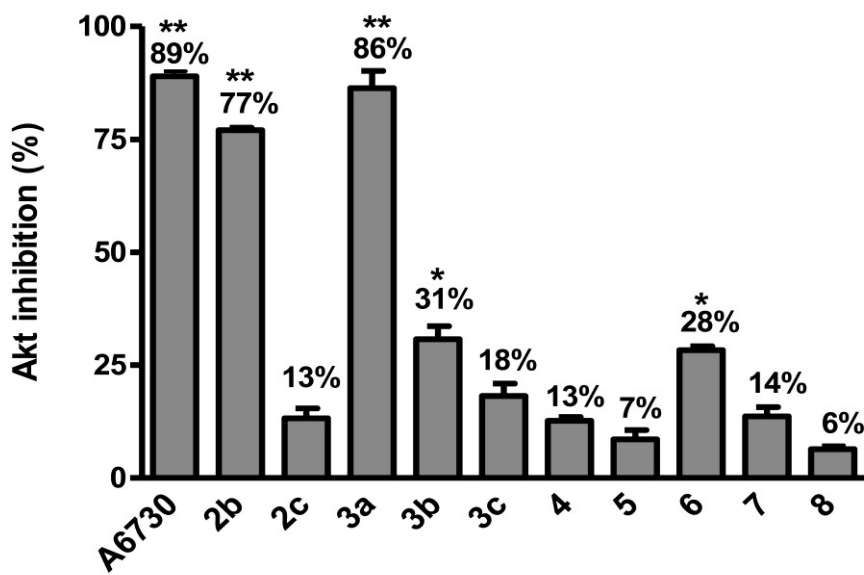


Figure 2

Moreover, the activity of **2c**, **3c** and **4** are comparable indicating that the short chains in **2c** and **3c** have poor influence. Finally the alkyl sulfoquinovosides **6** and **7** lacking the glycerol moiety exhibited a very low activity. The Akt1/2 kinase allosteric inhibitor (1,3-dihydro-1-(1-((4-(6-phenyl-1H-imidazo[4,5-g]quinoxalin-7-yl)phenyl)methyl)-4-piperidinyl)-2H-benzimidazol-2-one trifluoroacetate salt hydrate, indicated as A6730 from Sigma), included in ELISA studies as reference compound, showed 89% inhibition of Akt, demonstrating the strength of the test. For the compound **3a** a concentration-response analysis was performed (Figure 3). The compound showed a concentration-dependent significant inhibitory effect of Akt1 activity ($IC_{50} = 31.33 \mu\text{M}$, 95% confidence interval 21.18 – 45.71, $r^2 = 0.9484$). It is worthy of note that, with the same specific ELISA test [30], perifosine (a suggested Akt inhibitor targeting the PH domain) [31] displayed a similar inhibition with an IC_{50} value of $43.35 \mu\text{M}$, whereas the surfactant sodium dodecyl sulphate (SDS) didn't exhibit inhibition of Akt thus supporting a specific effect induced by **3a**.

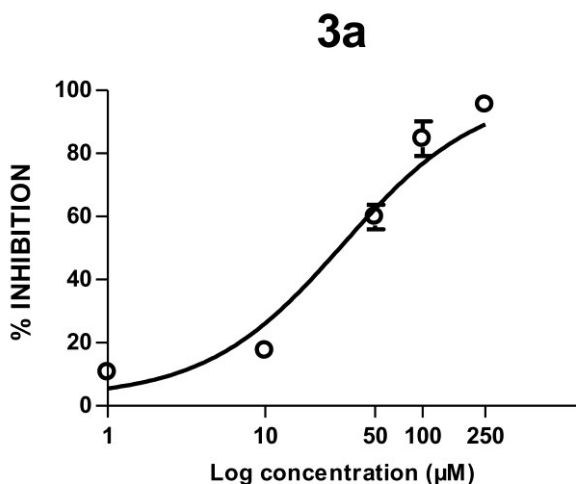


Figure 3

To evaluate the selectivity of compound **3a** against the Akt PH domain, we tested the effect on the activity of another kinase containing the PH domain, i.e., BTK (Bruton's tyrosine kinase). The results indicate that compound **3a** as well as the standard Akt1/2 inhibitor A6730 did not substantially affect the activity of such a kinase, suggesting that the effect on Akt is selective (Figure 4). On the contrary, the prototypical ATP-competitive kinase inhibitor staurosporine inhibited BTK activity (Figure 4) besides Akt activity (not shown).

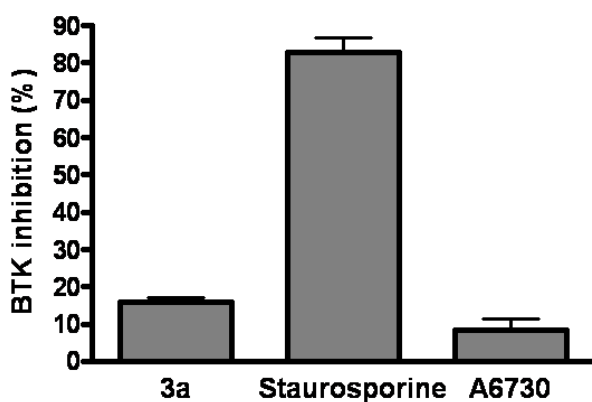


Figure 4

2.3 Docking studies

In an attempt to qualitatively define the mechanism by which the compounds tested *in vitro* could interact with Akt and inhibit its activity, docking simulations were carried out using the X-ray crystal structure of the PH domain of human Akt (PDB entry: 1UNQ, 0.98 Å resolution) [32]. To assess the docking procedure, we performed the first run of docking using 4IP (inositol-(1,3,4,5)-tetrakisphosphate) as the ligand (in the crystal structure of Akt, the protein is co-crystallized with this organic cofactor, PDB ID:1UNQ). Since all the studied compounds are phosphatidylinositol (PIs) analogues, we used as docking space all the spheres generated by DOCK6 program within 10Å of the PIs binding site. The anchor and growth procedure followed by the algorithm of DOCK6 program allowed initially the docking of the sugar ring. Hereafter, little segments of the acyl chains were added to the sugar ring, and minimized to obtain the lower energy possible. Despite the high conformational variability of the molecules due to the long acyl chains, the algorithm used in the docking procedure allowed us to obtain robust results and identify some key features of the substituted sugar ring necessary for an efficient binding. The resulting docking simulations poses are shown in Figure 5 and the relative Grid score docking energies in Suppl Table 1.

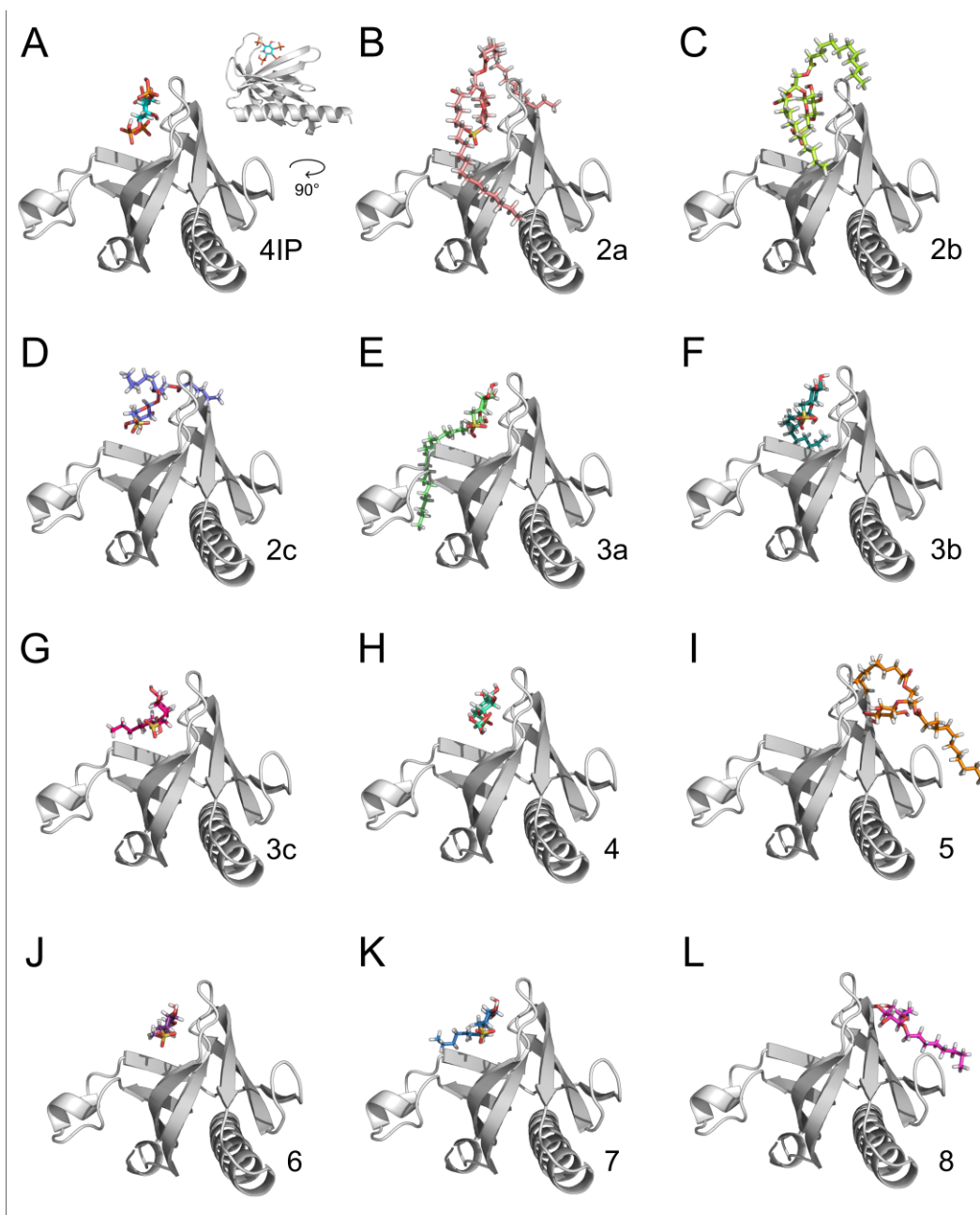


Figure 5

The interpretation of these results well fit with the experimental data obtained from ELISA tests. A structural difference between compounds **5** and **8** and the rest of the series is the lack of the functional group SO_3^- . Since compounds **5** and **8**, when compared with other molecules, are found to bind in a different position, the sulfonate group seems to be fundamental for the correct

binding of the molecule, and therefore for its biological activity. In particular the orientation of this group is in a zone of the protein surface rich in positively charged aminoacids (K14, R23, R25, Figure 6). Only compound **4** showed a different orientation of the SO_3^- group, and this observation could also explain the weak docking score of this compound with Akt. It must be underlined that also the length of the acyl chains plays a fundamental role in easing the binding of the compound. In fact, a longer chain appeared to provide a more stable interaction between Akt and the inhibitor than a shorter one (e.g., docking energy was -73.78 for the most active **3a** vs -59.51 and -51.00 Kcal/mol for the less active **3c** and **7**, see Figure 2 and Suppl Table 1).

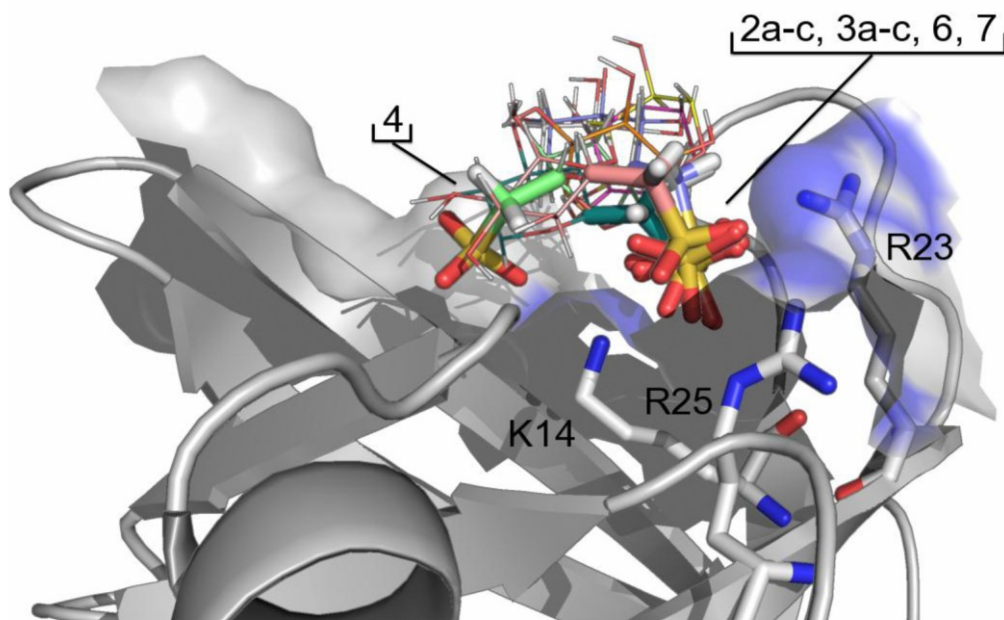


Figure 6

2.4 Cellular studies

ELISA assays and molecular modelling data highlighted compound **3a**, as a promising inhibitor of Akt in this series. To evaluate its potential as anticancer agent, the activity of compound **3a** was assayed in different cell lines in comparison with compounds **7** and **8** as

negative controls and the known Akt inhibitor A6730. Compound **2a** could not be tested also in cellular systems because of solubility limits. The used cell lines were endowed with an hyperactivated Akt and included murine *K-RAS*-transformed fibroblasts (NIH3T3 *K-RAS*) and human papillary thyroid carcinoma and ovarian carcinoma cell lines.

2.5 Akt phosphorylation inhibition studies on NIH 3T3 *K-RAS* cells

NIH3T3-*K-RAS* cells, expressing an activated form of the *K-RAS* gene and showing an hyperactivation on the Akt signalling pathway have been used as cellular model to investigate the effect of compounds on Akt phosphorylation under different conditions, i. e. serum-starvation, serum-stimulation and pre-treatment with selected inhibitors (see materials and methods). As reported in Figure 7, only compound **3a** displayed an inhibitory activity on Akt, both in pre-treated and in serum-stimulated cells. In agreement with docking studies and ELISA assays, compound **8** did not affect P-Akt and compound **7** appeared to be inactive. The results of the densitometric analysis are shown in Figure 7B, where the data are expressed as percentage of the respective control after the normalization versus actin and the calculation of the P-Akt/total Akt ratio. The data highlight the significant inhibition of the Akt activation induced by compound **3a** (about 40%). Neither compound **7** nor compound **8** exerted similar effect.

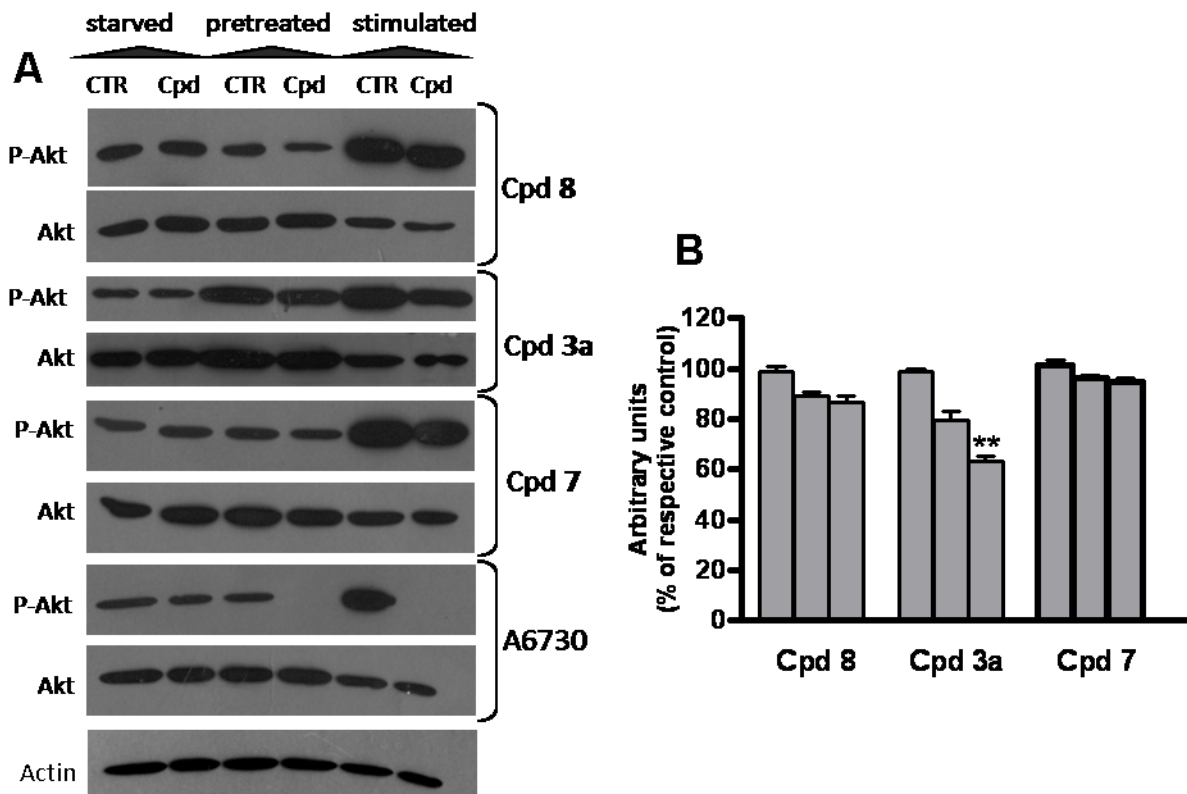


Figure 7

2.6 Papillary thyroid carcinoma and ovarian carcinoma cell growth inhibition

To further explore the features of compound **3a**, we examined the growth inhibitory effect on human tumor cell lines in which Akt signaling is known to play a role. Aberrant activation of the PI3K/Akt pathway plays a fundamental role in the tumorigenesis and progression of thyroid cancers [33]. The major oncogenic mutations found in papillary thyroid carcinomas (PTCs) involving BRAF, RAS, PI3KCA, RET genes have been demonstrated to activate the PI3K/Akt pathway. Thus, targeting this deregulated signaling cascade represents an attractive therapeutic approach for treatment of PTC tumors. Moreover, it has been reported that thyroid cancer cells characterized by PI3K/Akt signaling deregulation show a preferential sensitivity to inhibitors of

this pathway [34]. On these bases, we tested the antiproliferative activity of sulfoglycolipids **3a**, including compounds **7** and **8** as negative controls, on three PTC cell lines characterized by constitutive activation of the Akt pathway functionally related to RET/PTC-1 rearrangement (TPC-1 cells), to PI3KCA gene E542K mutation (K1 cells), and to decreased expression of the dual-specificity phosphatase PTEN (Nim-1 cells). A 72h-treatment with compound **3a** induced a concentration-dependent inhibition of PTC cell growth. The inhibitory effect (about 30%) at the highest concentration tested (50 μ M) was significant in TPC-1 and K1 cells ($p < 0.05$ and $p < 0.007$ versus untreated control, respectively) (Figure 8A). K1 cells treated with 50 μ M **3a** displayed signs of cytotoxicity such as vacuolated and granulated cytoplasm (not shown). Compounds **7** and **8** did not induce a significant inhibition of PTC cell growth after 72h. The Akt1/2 kinase allosteric inhibitor (A6730), included in this studies as reference compound, showed a comparable antiproliferative activity on TPC-1 and K1 cells ($IC_{50} = 11 \pm 1.6 \mu$ M and $IC_{50} = 10 \pm 5 \mu$ M, respectively). Of note, Nim-1 cells were the most sensitive to this inhibitor ($IC_{50} = 3 \pm 1.6 \mu$ M) in keeping with data describing an increased sensitivity of PTEN-deficient cells to PI3K/Akt inhibitors [35].

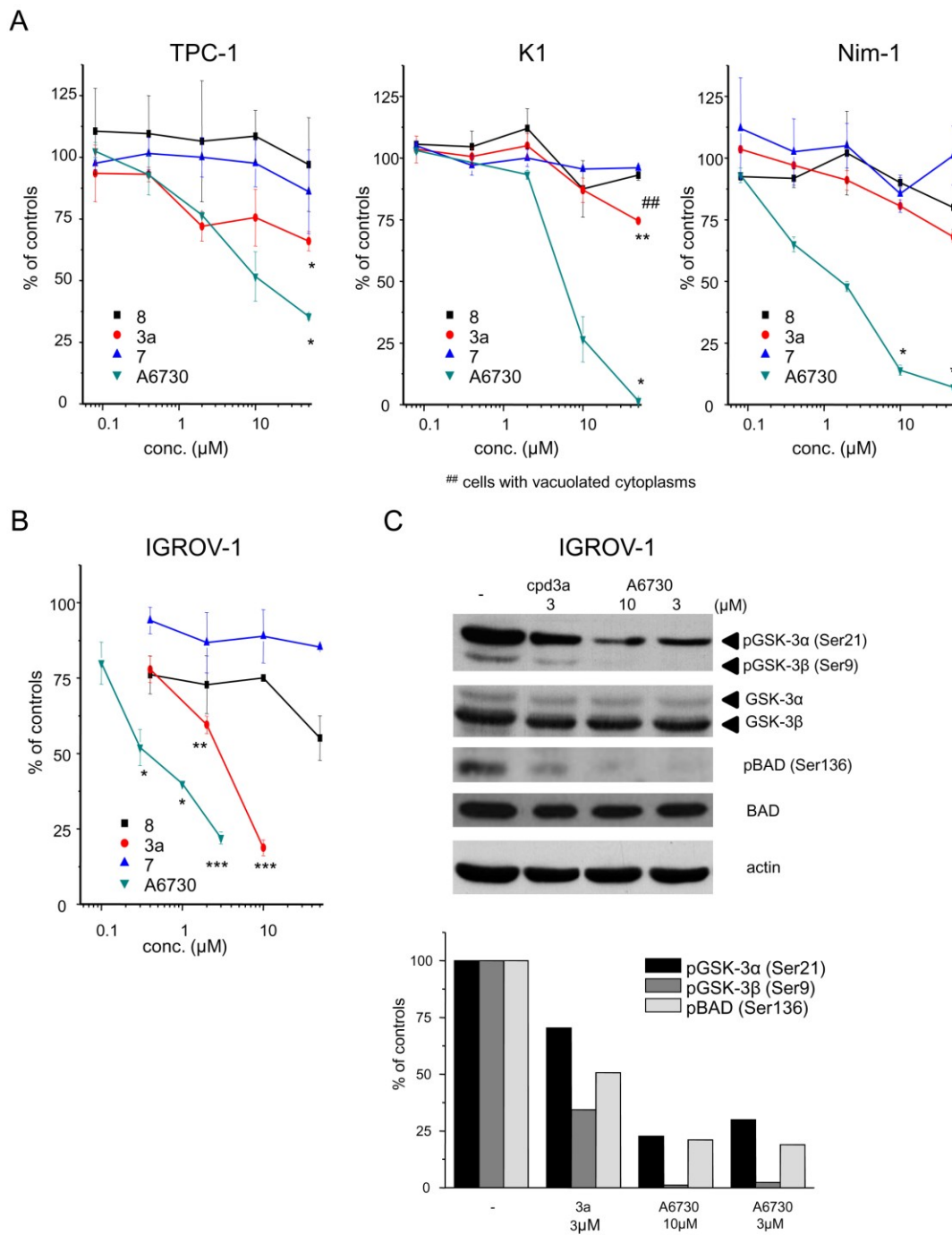


Figure 8

Next, the efficacy of the sulfoglycolipids compounds was assessed on the ovarian carcinoma cell line IGROV-1 previously described as PI3K-addicted [36]. To facilitate drug uptake and interaction with the target, cells were treated in the absence of serum. In this model, compound **3a** effectively reduced cell growth in a concentration-dependent manner with an IC_{50} of 2 ± 1.4 μ M, whereas compound **7** was substantially inactive, and compound **8** slightly affected cell proliferation (Figure 8B). Thus, only, compound **3a** exhibited a biological effect in the cellular tests. The IGROV-1 cell line showed a high sensitivity to the reference compound ($IC_{50} = 0.3 \pm 0.15$ μ M) according with the relevance of the Akt pathway in mediating cell proliferation. Biochemical analysis performed on whole IGROV-1 cell lysates confirmed the ability of **3a** to affect PI3K/Akt signaling after 24h of treatment. Indeed, a reduced serine phosphorylation of the critical Akt downstream substrates GSK-3 α and β [37], and BAD was observed in cells exposed to a **3a** concentration in the range of IC_{50} (3 μ M) (Figure 8C). This finding supports the ability of this sulfoglycolipid to affect target activation and confirm the compound ability to enter the cells. Again, the standard Akt1/2 inhibitor was highly effective in inhibiting Akt downstream effects.

3. Conclusions

In the present work, we show that synthetic sulfo-glycoconjugates derived from a D-glucosidic scaffold, designed to mimic phosphatidyl inositols are able to impair Akt kinase activity. The synthesized compounds were tested both in ELISA assays with purified Akt and in different cell lines characterized by Akt hyperactivation. Docking studies and ELISA assay evidenced that the longer the acyl chain, the better is the activity, while an acidic anionic group is fundamental to guarantee optimal electrostatic interactions within the binding pocket. Compound **3a**, endowed with these features, showed selectivity for Akt and biological activity in

the tested cellular systems. This compound is a promising candidate, useful as lead compound for the design of more efficient inhibitors of Akt, taking into consideration key structural features of the studied sulfoglycolipids and chemico-physical properties favouring solubility and cell permeability.

4. Experimental

4.1 Chemistry

Methyl 2,3,4-tri-*O*-acetyl-6-*O*-tosyl- β -D-glucopyranoside (**9**) was synthesized according to the literature procedure [29]. Octyl β -D-glucopyranoside was purchased from Aldrich. Optical rotations were determined on a Perkin–Elmer 241 polarimeter at 20 °C, in a 1 dm cell. Melting points were recorded on a Büchi 510 capillary melting point apparatus and were uncorrected. All reagents and solvents used were reagent grade and were purified before use by standard methods. Dry solvents and liquid reagents were distilled prior to use or dried on 4 Å molecular sieves. Column chromatography was carried out on flash silica gel (Merck 230–400 mesh). TLC analysis was carried out on silica gel plate (Merck 60F254) with detection by charring with 50% sulfuric acid or anisaldehyde based reagent. Evaporation under reduced pressure was usually performed below 40 °C otherwise specified. The structures of all the new synthesized compounds were confirmed through full ^1H and ^{13}C NMR characterization and mass spectroscopy. ^1H NMR analysis were performed at 500 MHz with a Bruker FT-NMR AVANCE™ DRX500 spectrometer using a 5 mm z-PFG (pulsed field gradient) broadband reverse probe at 298 K unless otherwise stated, and ^{13}C NMR spectra at 125.76 MHz were done of all the new compounds. The signals were unambiguously assigned by 2D COSY and HSQC

experiments (standard Bruker pulse program). Chemical shifts are reported as δ (ppm) relative to residual CHCl_3 or CH_3OD fixed at 7.24 and 3.30 ppm, respectively, for ^1H NMR spectra and relative to CDCl_3 fixed at 77.0 ppm (central line) or CD_3OD at 49.00 ppm (central line) for ^{13}C NMR spectra; scalar coupling constants are reported in hertz. Mass spectra were recorded in negative or positive-ion electrospray (ESI) mode on a Thermo Quest Finnigan LCQ DECA™ ion trap mass spectrometer; the mass spectrometer was equipped with a Finnigan ESI interface; sample solutions were injected with a ionization spray voltage of 4.5 kV or 5.0 kV (positive and negative-ion mode, respectively), a capillary voltage of 32 V or -15 V (positive and negative-ion mode, respectively), and capillary temperature of 250 °C. Data were processed by Finnigan Xcalibur software system. TLC, NMR and MS confirmed purity and identity of all synthesized compounds. High resolution mass spectra (HRMS) of the new target compounds (**4** and **6-8**) were also recorded at C.I.G.A. (Centro Interdipartimentale Grandi Attrezzature, University of Milan) on a Fourier Transform Ion Cyclotron Resonance (FT-ICR) mass spectrometer APEX II & Xmass software (Bruker Daltonics) – 4.7 T magnet (Magnex), in positive-ion electrospray (ESI) mode. Samples were injected as <1 to 5 $\mu\text{g}/\text{mL}$ methanol solutions and eluted with methanol (120 $\mu\text{L}/\text{h}$).

4.2 Synthesis of 2-O- β -D-sulfoquinovopyranosyl-sn-glycerol potassium salt **4**.

To a solution of **3a** (0.041 g, 0.066 mmol) in methanol (0.5 mL) 0.1 mL of 0.7 M sodium methoxide in methanol were added. The reaction was monitored by TLC (AcOEt:*i*PrOH:H₂O 3:3:1 v/v) and after 4 h was neutralized with DOWEX-50 x 8H⁺. The resin was filtered and the solvent dried under vacuum. Water (3 mL) was added and extracted with petroleum ether (1.5 mL x 2). The acidic water solution was then neutralized with 0.1 M KOH and washed again with

chloroform to remove the remaining traces of stearic acid. Water was dried by freeze-drying to obtain 0.017 g of the potassium salt **4** (0.046 mmol, 71% yield, hygroscopic). ^1H NMR (D_2O): δ = 3.49 (dd, $J_{5',6'a} = 9.7$ Hz, $J_{6'a,6'b} = 14.8$ Hz, 1H, H-6'a), 3.70 (dd, $J_{3',4'} = 9.3$ Hz, $J_{4',5'} = 9.5$ Hz, 1H, H-4'), 3.75 (dd, $J_{1',2'} = 8.0$ Hz, $J_{2',3'} = 9.3$ Hz, 1H, H-2'), 3.82 (dd, $J_{5',6'b} = 1.7$ Hz, 1H, H-6'b), 3.93 (dd, 1H, H-3'), 4.10-4.21 (m, 4H, H-1a, H1b, H3a and H3b), 4.22 (ddd, 1H, H-5'), 4.32 (m, 1H, H-2), 5.03 (d, 1H, H-1'). ^{13}C NMR (D_2O): δ = 52.16 (C6'), 60.99 (C3 or C1), 61.14 (C1 or C3), 72.21 (C5'), 72.41 (C4'), 73.22 (C2'), 75.38 (C3'), 81.11 (C2), 101.95 (C1'). ESI-MS (CH_3OH , negative-ion mode): $m/z = 317.1$ [M-K]. Calcd for $\text{C}_9\text{H}_{17}\text{O}_{10}\text{SK}$, m/z 356.02 [M]. ESI-HRMS (CH_3OH , negative-ion mode): $m/z = 317.05451$ [M-K] (error, 0.9 ppm). Calcd for $\text{C}_9\text{H}_{17}\text{O}_{10}\text{S}$, $m/z = 317.05479$ (monoisotopic mass).

4.3 Synthesis of the sulfonates **6** and **7**

Methyl 2,3,4-tri-O-acetyl-6-deoxy-6-thioacetyl- β -D-glucopyranoside 10. The known tosyl **9** (0.10 g, 0.211 mmol) was dissolved in dry DMF (3 mL), and potassium thioacetate (0.08 g, 0.7 mmol) was added. The mixture was stirred overnight under an atmosphere of Ar at room temperature. After disappearing of the starting material as shown by TLC (petroleum ether:ethyl acetate 50:50 v/v) water (7 mL) was added and extracted with dichloromethane (20 mL x 3). The collected organic layers were washed with water (10 mL x 2), dried with sodium sulphate and concentrated under vacuum. DMF was co-evaporated with cyclohexane at reduced pressure at 45-50 °C. Subsequent flash chromatography (petroleum ether:ethyl acetate 60:40 v/v) of the crude residue yielded the desired derivative **10** (0.075 g, 0.2 mmol, 94% yield). Mp: 91-92°C (amorphous solid); $[\alpha]_D^{20} = -19.3$ (CH_2Cl_2 , $c=1.1$). ^1H NMR (CDCl_3): δ = 1.93, 1.98 and 2.01 (3s, 9H, 3 CH_3CO), 2.28 (s, 3H, CH_3COS), 3.00 (dd, 1H, $J_{5,6a} = 7.0$ Hz, $J_{6a,6b} = 14.3$ Hz, 1H, H-6a), 3.20

(dd, 1H, $J_{5,6b} = 3.0$ Hz, 1H, H-6b), 3.43 (s, 3H, OCH₃), 3.56 (ddd, $J_{4,5} = 9.5$ Hz, 1H, H-5), 4.33 (d, $J_{1,2} = 8.0$ Hz, 1H, H-1), 4.88 (dd, $J_{2,3} = 9.5$ Hz, 1H, H-2), 4.90 (dd, $J_{3,4} = 9.5$ Hz, 1H, H-4), 5.11 (dd, 1H, H-3). ¹³C NMR (CDCl₃): $\delta = 20.49$ (CH₃CO), 20.59 (2CH₃CO), 30.01 (C6), 30.29 (CH₃COS), 56.76 (OCH₃), 70.56 (C4), 71.14 (C2), 72.63 (C3), 72.78 (C5), 101.23 (C1), 169.28, 169.64 and 170.12 (3CO), 194.60 (SCO). ESI-MS (CH₃OH, positive-ion mode): $m/z = 401.0$ [M+Na]⁺. Calcd for C₁₅H₂₂O₉S, m/z 378.1 [M].

Methyl 2,3,4-tri-O-acetyl- β -D-sulfoquinovopyranoside 11

Potassium monopersulfate triple salt (Oxone[®], 0.182 g, 0.296 mmol) and potassium acetate (0.281 g, 2.87 mmol) were added in that order to a solution of compound **10** (0.075 g, 0.198 mmol) in glacial acetic acid (2.5 mL). The suspension was stirred at room temperature overnight after checking by TLC (petroleum ether:ethyl acetate 50:50 v/v and CH₂Cl₂:CH₃OH 80:20 v/v) and another amount of the oxidant was added (0.182 g, 0.296 mmol). The solvent was dried under vacuum and the crude residue was submitted twice to flash chromatography purification (CH₂Cl₂:CH₃OH 90:10 to 80:20 v/v) yielding 0.073 g (0.19 mmol, 96% yield) of **11**. Mp: 167-173°C dec; $[\alpha]_D^{20} = -1.7$ (CH₃OH, $c=1.0$). ¹H NMR (CD₃OD): $\delta = 1.95$, 2.00 and 2.03 (3s, 9H, 3CH₃CO), 3.01 (dd, 1H, $J_{5,6a} = 5.2$ Hz, $J_{6a,6b} = 15.0$ Hz, 1H, H-6a), 3.03 (dd, 1H, $J_{5,6b} = 5.2$ Hz, 1H, H-6b), 3.50 (s, 3H, OCH₃), 4.07 (ddd, $J_{4,5} = 9.5$ Hz, 1H, H-5), 4.55 (d, $J_{1,2} = 8.0$ Hz, 1H, H-1), 4.86 (dd, $J_{3,4} = 9.5$ Hz, 1H, H-4), 4.87 (dd, $J_{2,3} = 9.5$ Hz, 1H, H-2), 5.23 (dd, 1H, H-3). ¹³C NMR (CD₃OD): $\delta = 18.52$, 18.59 and 18.67 (3CH₃CO), 51.62 (C6), 55.48 (OCH₃), 69.68 (C5), 70.77 (C4), 70.97 (C2), 72.40 (C3), 100.46 (C1), 169.25, 169.54 and 169.63 (3CO). ESI-MS (CH₃OH, negative-ion mode): $m/z = 382.9$ [M-1]⁻. Calcd for C₁₃H₂₀O₁₁S, m/z 384.07 [M].

Methyl β -D-sulfoquinovopyranoside potassium salt 6

To a methanol solution (1.0 mL) of triacetate **11** (0.073 g, 0.19 mmol), 0.54 mL of 1M sodium methoxide in methanol were added and the reaction was stirred at room temperature for 5 h

(TLC, CH₂Cl₂:CH₃OH 80:20 v/v and AcOEt:iPrOH:H₂O 3:3:1 v/v). After neutralizing with DOWEX-50 x 8H⁺ the resin was filtered and the solvent dried under vacuum. Water (2 mL) was added and the acidic solution was neutralized with 0.1 M KOH. To decolorize the yellowish solution, it was diluted with 10 mL of methanol and water (1.5 mL) and refluxed with activated charcoal. The solvent was reduced under vacuum, water was added (1 mL) and dried by freeze-drying to obtain **6** (0.046 g, 0.15 mmol, 82% yield, hygroscopic) as potassium salt. $[\alpha]_D^{20} = -6.4$ (D₂O, c=0.9). ¹H NMR (D₂O): $\delta = 2.93$ (dd, 1H, $J_{5,6a} = 9.7$ Hz, $J_{6a,6b} = 14.8$ Hz, 1H, H-6a), 3.13 (dd, $J_{3,4} = 9.4$ Hz, $J_{4,5} = 9.4$ Hz, 1H, H-4), 3.15 (dd, $J_{1,2} = 8.0$ Hz, $J_{2,3} = 9.3$ Hz, 1H, H-2), 3.28 (dd, 1H, $J_{5,6b} = 1.4$ Hz, 1H, H-6b), 3.37 (dd, 1H, H-3), 3.42 (s, 3H, OCH₃), 3.65 (ddd, 1H, H-5), 4.24 (d, 1H, H-1). ¹³C NMR (D₂O): $\delta = 51.97$ (C6), 57.10 (OCH₃), 72.05 (C5), 72.32 (C4), 73.06 (C2), 75.54 (C3), 102.97 (C1). ESI-MS (CH₃OH, negative-ion mode): $m/z = 257.2$ [M-K]. Calcd for C₇H₁₃O₈SK, $m/z 296.00$ [M]. ESI-HRMS (CH₃OH, negative-ion mode): $m/z = 257.03332$ [M-K] (error, 1.3 ppm). Calcd for C₇H₁₃O₈S, $m/z = 257.03366$ (monoisotopic mass).

Octyl 2,3,4-tri-O-acetyl-6-O-tosyl- β -D-glucopyranoside 12

Tosyl chloride (0.76 g, 4.0 mmol) was added to a solution of octyl β -D-glucopyranoside (1g, 3.42 mmol) in pyridine (22 mL) at -5°C and left overnight at this temperature. After about 90% conversion of the starting material as shown by TLC (ethyl acetate 100%), acetic anhydride (4.85 mL, 51.3 mmol) was added at 0°C under stirring. After 1 h the reaction mixture was left to gradually reach the room temperature. After 4 h the reaction was completed (TLC, petroleum ether:ethyl acetate 60:40 v/v), then poured into ice/water (100 mL) and extracted with dichloromethane (30 mL x 5). The collected organic layers were then washed with 5M hydrochloric acid (35 mL x 2), sodium bicarbonate (50 mL) and water (50 mL x 2), dried with sodium sulphate and concentrated under reduced pressure. Crystallization of the crude material (1.87 g) with a mixture of ethanol (18 mL) and dichloromethane (1 mL) yielded 1.332 g (2.33

mmol, 68% yield) of pure **12**. Mp: 109-110°C; $[\alpha]_D^{20} = -4.6$ (CHCl₃, c=1.0); ¹H NMR (CDCl₃): $\delta = 0.86$ (t, J= 6.7, 3H, CH₃), 1.18-1.33 (m, 10H, 5 CH₂), 1.50 (m, 2H, CH₂), 1.96, 1.97 and 1.99 (3s, 9H, 3 CH₃CO), 2.43 (s, 3H, CH₃), 3.39 (m, 1H, OCHa), 3.71 (m, 1H, H-5), 3.75 (m, 1H, OCHb), 4.04 (dd, J_{5,6a} = 5.9 Hz, J_{6a,6b} = 10.9 Hz, 1H, H-6a), 4.09 (dd, J_{5,6b} = 3.0 Hz, 1H, H-6b), 4.41 (d, J_{1,2} = 7.9 Hz, 1H, H-1), 4.86 (dd, J_{2,3} = 9.5 Hz, 1H, H-2), 4.87 (dd, J_{3,4} = 9.5 Hz, J_{4,5} = 9.7 Hz, 1H, H-4), 5.14 (dd, 1H, H-3). ¹³C NMR (CDCl₃): $\delta = 14.03$ (CH₃), 20.50, 20.54 and 20.55 (3 CH₃CO), 21.62 (CH₃Ph), 22.61 (CH₂), 25.80 (CH₂), 29.22 (CH₂), 29.24 (CH₂), 29.35 (CH₂), 31.77 (CH₂), 67.91 (C6), 68.87 (C4), 70.15 (OCH₂), 71.23 (C2), 71.58 (C5), 72.62 (C3), 100.60 (C1), 128.05 (2 CHPh), 129.86 (2 CHPh), 132.59 (CPh), 145.08 (CPh), 169.14, 169.46 and 170.16 (3 CO). ESI-MS (CH₃OH, positive-ion mode): m/z = 595.0 [M+Na]⁺. Calcd for C₂₇H₄₀O₁₁S, m/z 572.23 [M].

Octyl 2,3,4-tri-O-acetyl-6-deoxy-6-thioacetyl- β -D-glucopyranoside 13

Compound **12** (0.50 g, 0.87 mmol) was dissolved in dry DMF (4 mL), and potassium thioacetate (0.360 g, 3.15 mmol) was added. The mixture was stirred under Ar at room temperature and the progress of the reaction was monitored by TLC (petroleum ether:ethyl acetate 70:30 v/v). After 6 h the reaction was stopped and after water (9 mL) addition extracted with dichloromethane (30 mL x 3). The collected organic layers were washed with water (10 mL x 2), dried with sodium sulphate and concentrated under vacuum. DMF was co-evaporated with cyclohexane at reduced pressure at 45-50 °C and subsequent flash chromatography (petroleum ether:ethyl acetate 80:20 v/v) of the crude derivative **13** was obtained (0.396 g, 0.832 mmol, 95% yield). Mp: 58-59°C (wax); $[\alpha]_D^{20} = -10.4$ (CHCl₃, c=1.0). ¹H NMR (CDCl₃): $\delta = 0.84$ (t, J= 6.9, 3H, CH₃), 1.17-1.33 (m, 10H, 5 CH₂), 1.52 (m, 2H, CH₂), 1.95, 1.98 and 2.04 (3s, 9H, 3 CH₃CO), 2.30 (s, 3H, CH₃COS), 3.00 (dd, J_{5,6a} = 7.1 Hz, J_{6a,6b} = 14.2 Hz, 1H, H-6a), 3.22 (dd, J_{5,6b} = 3.0 Hz, 1H, H-6b), 3.43 (m, 1H, OCHa), 3.56 (ddd, J_{4,5} = 10.0 Hz, 1H, H-5), 3.79 (m, 1H, OCHb), 4.41 (d, J_{1,2} = 8.0

Hz, 1H, H-1), 4.90 (dd, $J_{2,3} = 9.6$ Hz, 1H, H-2), 4.92 (dd, $J_{3,4} = 9.6$ Hz, 1H, H-4), 5.13 (dd, 1H, H-3). ^{13}C NMR (CDCl_3): $\delta = 14.01$ (CH_3), 20.55 (2 CH_3CO), 20.63 (CH_3CO), 22.59 (CH_2), 25.77 (CH_2), 29.20 (CH_2), 29.38 (CH_2), 30.22 (C6), 30.32 (CH_3COS), 31.76 (CH_2), 70.04 (OCH_2), 70.85 (C4), 71.46 (C2), 72.81 (C3), 72.97 (C5), 100.62 (C1), 169.18, 169.67 and 170.20 (3 CO), 194.62 (SCO). ESI-MS (CH_3OH , positive-ion mode): $m/z = 499.0$ [$\text{M}+\text{Na}$] $^+$. Calcd for $\text{C}_{22}\text{H}_{36}\text{O}_9\text{S}$, m/z 476.21 [M].

Octyl 2,3,4-tri-O-acetyl- β -D-sulfoquinovopyranoside 14

Potassium monopersulfate triple salt (Oxone[®], 2.0 g, 3.26 mmol) and potassium acetate (1.12 g, 11.7 mmol) were added in that order to a solution of compound **13** (0.389 g, 0.817 mmol) in glacial acetic acid (15 mL). The suspension was stirred at room temperature and the reaction was monitored by TLC (petroleum ether:ethyl acetate 70:30 v/v and CH_2Cl_2 : CH_3OH 90:10 v/v). After disappearing of the starting material, the solvent was evaporated under vacuum, 5 M hydrochloric acid (40 mL) was added and extracted with dichlorometane (20 mL x 5). The collected organic layers were dried under vacuum and the crude residue purified by flash chromatography (CH_2Cl_2 : CH_3OH 90:10 to 80:20 v/v) yielding 0.352g (0.73 mmol, 89% yield) of compound **14** as a white foam. $[\alpha]_D^{20} = -16.8$ (CH_3OH , $c=1.0$). ^1H NMR (CD_3OD): $\delta = 0.89$ (t, $J = 6.9$, 3H, CH_3), 1.25-1.35 (m, 10H, 5 CH_2), 1.54 (m, 2H, CH_2), 1.95, 2.00 and 2.02 (3s, 9H, 3 CH_3CO), 3.02 (dd, $J_{5,6a} = 5.0$ Hz, $J_{6a,6b} = 14.8$ Hz, 1H, H-6a), 3.03 (dd, $J_{5,6b} = 5.0$ Hz, 1H, H-6b), 3.52 (m, 1H, OCHa), 3.92 (m, 1H, OCHb), 4.06 (ddd, $J_{4,5} = 10.0$ Hz, 1H, H-5), 4.62 (d, $J_{1,2} = 8.0$ Hz, 1H, H-1), 4.86 (dd, $J_{3,4} = 9.6$ Hz, 1H, H-4), 4.87 (dd, $J_{2,3} = 9.6$ Hz, 1H, H-2), 5.23 (dd, 1H, H-3). ^{13}C NMR (CD_3OD): $\delta = 12.40$ (CH_3), 18.53, 18.65 and 18.69 (3 CH_3CO), 21.69, 25.03, 28.40, 28.43, 28.49 and 30.96 (6 CH_2), 51.77 (C6), 68.98 (OCH_2), 69.63 (C5), 70.85 (C4), 71.11 (C2), 72.39 (C3), 99.60 (C1), 169.13, 169.56 and 169.65 (3 CO). ESI-MS (CH_3OH , negative-ion mode): $m/z = 481.1$ [$\text{M}-1$] $^-$. Calcd for $\text{C}_{20}\text{H}_{34}\text{O}_{11}\text{S}$, m/z 482.18 [M].

Octyl β-D-sulfoquinovopyranoside potassium salt 7

To a methanol solution (2.0 mL) of triacetate **14** (0.352 g, 0.73 mmol), 2.6 mL of 1M sodium methoxide in methanol were added and, following the procedure described for compound **6**, the reaction was stirred at room temperature overnight (TLC, CH₂Cl₂:CH₃OH 80:20 v/v and AcOEt:*i*PrOH:H₂O 3:3:1 v/v). After neutralizing with DOWEX-50 x 8H⁺ the resin was filtered and the solvent dried under vacuum. Water (1 mL) was added and the acidic solution was neutralized with 0.4 M KOH. To decolorize the yellowish solution, it was diluted with 6 mL of methanol and refluxed with activated charcoal. The solvent was reduced under vacuum, water was added (1 mL) and dried by freeze-drying to obtain **7** (0.234 g, 0.59 mmol, 81% yield) as potassium salt. Mp: 155-160°C dec; $[\alpha]_D^{20} = -3.9$ (D₂O, c=1.8). ¹H NMR (D₂O): $\delta = 0.78$ (t, J= 6.9, 3H, CH₃), 1.14-1.31 (m, 10H, 5 CH₂), 1.54 (m, 2H, CH₂), 2.97 (dd, J_{5,6a} = 9.5 Hz, J_{6a,6b} = 14.8 Hz, 1H, H-6a), 3.18 (dd, J_{3,4} = 9.2 Hz, J_{4,5} = 9.5 Hz, 1H, H-4), 3.19 (dd, J_{1,2} = 8.0 Hz, J_{2,3} = 9.2 Hz, 1H, H-2), 3.31 (dd, J_{5,6b} < 1.0 Hz, 1H, H-6a), 3.41 (dd, 1H, H-3), 3.57 (m, 1H, OCHa), 3.68 (ddd, 1H, H-5), 3.83 (m, 1H, OCHb), 4.36 (d, 1H, H-1). ¹³C NMR (D₂O): $\delta = 13.44$ (CH₃), 22.04, 25.12, 28.42, 28.49, 28.69 and 31.12 (6 CH₂), 52.17 (C6), 70.63 (OCH₂), 72.12 (C5), 72.45 (C4), 73.22 (C2), 75.74 (C3), 102.00 (C1). ESI-MS (CH₃OH, negative-ion mode): m/z = 355.2 [M-K]. Calcd for C₁₄H₂₇O₈SK, m/z 394.11 [M]. ESI-HRMS (CH₃OH, negative-ion mode): m/z = 355.14257 [M-K] (error, 1.8 ppm). Calcd for C₁₄H₂₇O₈S, m/z = 355.14321 (monoisotopic mass).

4.4 Docking Studies

Docking studies were performed using the high resolution X-ray structure of PH domain of Protein kinase B/Akt (pdb entry: 1UNQ [Milburn, C.C]). Ligands structures were built using the chemistry package Molecular Operating Environment (MOE) [Chemical Computing Group Inc.

<http://www.chemcomp.com/>]. Receptors and ligand atom types and charges were calculated using the AM1-BCC method of the antechamber package, available in the software UCSF Chimera [38], in order to recognize atom and bond types, generating the residue topology file and finding force field parameters. Docking simulations were performed using DOCK6 [39]. Starting from receptor surface, spheres with a maximum radius of 3 Å and a minimum radius of 1 Å were generated. The ensemble of spheres within 10Å of the bounded inositol-(1,3,4,5)-tetrakisphosphate (4IP) molecule was assumed to represent the binding site core, and box in which poses were generated was built extending the binding site core by additional 10Å along the Cartesian axes. The grid was calculated including all receptor atoms and the distance between grid point along each axes was of 0.3 Å. Non polar hydrogen atoms were modeled using the all atom model: hydrogens attached. During dock calculations, ligands were kept flexible and 500 minimization cycle were performed both for the anchor (the largest rigid substructure of the ligand) and the branches (other component of the ligand molecules). Very similar poses (RMSD < 0,1) were clustered and the best 30 poses were ranked according to Grid Score (score is given by approximate molecular mechanics interaction energies, consisting of van der Waals and electrostatics components without solvation energy) [39]. When considering very flexible molecules, such as **2a**, several conformations (differing only for small differences in the orientation of the alkyl chains) clustered within a narrow energy range. However, for the sake of clarity, only the lowest energy poses are presented and discussed.

4.5 Biological Assays

4.5.1 Akt inhibition assays

ELISA test. The Akt kinase activity assay was performed by employing a commercial ELISA kit designed specifically to screen inhibitors or activators of Akt. The inhibitory activity of compounds was tested employing the CycLex AKT/PKB kinase Assay/Inhibitor Screening Kit (CycLex, Eppendorf, Milano, Italy). Plates were pre-coated with “AKTide-2T” which can be efficiently phosphorylated by Akt1. The detector antibody specifically detects the phosphorylated “AKTide-2T”. Particularly, to perform the test, the samples were dissolved in DMSO (except for **4** which was dissolved in distilled water), and diluted in Kinase Buffer to a final concentration of 100 μM . For compound **3a**, a concentration-response analysis was also performed employed a concentration range of 1-250 μM . Compounds were added together with constitutive active form of human Akt1 (25 m units/well), and allowed to phosphorylate the bound substrate following the addition of Mg^{2+} and ATP. The amount of phosphorylated substrate was measured by binding it with horseradish peroxidase conjugate of an anti-phospho-AKTide-2T monoclonal antibody, which then catalyzes the conversion of the chromogenic substrate tetra-methylbenzidine from the colourless reduced form to the yellow oxidized product, after the addition of the stopping reagent. The absorbance of the resulting solution is determined spectrophotometrically at $\lambda_{\text{max}} = 450 \text{ nm}$, and it is related to Akt1 activity in the tested solution. The test was performed three times, each time in triplicate. As reference compound, the Akt1/2 kinase inhibitor (1,3-Dihydro-1-(1-((4-(6-phenyl-1H-imidazo[4,5-g]quinoxalin-7-yl)phenyl)methyl)-4-piperidinyl)-2H-benzimidazol-2-one trifluoroacetate salt hydrate, indicated as A6730 from Sigma, St. Louis, MO) was also used. Furthermore Staurosporine (Sigma-Aldrich, Milano, Italy) at the final concentration of 1 μM was employed as “inhibitor control” as indicated in the assay protocol to verify the function of the kit. Statistical analyses were performed using Kruskal-Wallis non parametric ANOVA. A value of $p < 0.05$ was considered statistically significant. The IC_{50} value is calculated through the GraphPad software.

BTK assay. The BTK kinase activity assay was performed by employing a commercial ADP-Glo™ Kinase Assay (Promega), a luminescent assay that measures ADP formed from a kinase reaction. The compounds were dissolved in DMSO and used at a final concentration of 100 μM. Compound **3a** was added together with BTK, and allowed to phosphorylate the substrate following the addition of ATP. The kinase reaction was performed according to the manufacturer's instructions. The test was performed twice, each time in triplicate. As reference compound, the Akt1/2 kinase inhibitor A6730 was used. Staurosporine was employed as positive control as indicated in the assay protocol.

Western blot analysis. NIH 3T3 cells transformed by an activated form of the K-ras oncogene (NIH 3T3 K-ras) [40] were grown at 37 °C in Dulbecco's modified Eagle's medium (DMEM) (Euroclone) supplemented with 10% heat-inactivated NBCS (Gibco-BRL). 3×10^5 cell/mL cells were plated in 12 well plates and starved for 16h in DMEM supplemented with 0.5% NCS. Cells were pre-treated with the different compounds at 100 μM or with vehicle (DMSO) for 1 h and then incubated in DMEM supplemented with 10% serum (NCS) for additional 30 min. Cell were then harvested and lysed in Lysis Buffer (50 mM Tris-HCl, pH 7.4, 5% glycerol, 200 mM NaCl, 1% IGEPAL (Sigma), 1 μM aprotinin, 1 μM leupeptin and 1 mM PMSF). Equal amounts of total protein extracts (15 μg) were loaded onto a 8% SDS-polyacrylamide gel and blotted to nitrocellulose membranes. Western blots were probed with anti-phospho-Akt (Ser 473) (Cell Signaling) antibodies; subsequently, filters were stripped and re-probed with anti-Akt (Cell Signaling) antibodies. Anti-actin antibody produced in rabbit (Sigma-Aldrich) was used as loading control. Secondary antibodies conjugated to horseradish peroxidase (HRP) (GE Healthcare) were used. All signals were detected after the HRP was activated by enhanced chemiluminescence.

4.5.2 Cellular Studies

Compound solution preparation. Compound **3a** and **7** were easily dissolved in 100% DMSO at 10 mM, whereas compound **8** was dissolved in 100% DMSO at the same concentration after prolonged stirring. A6730 (Sigma-Aldrich, St. Louis, MO) used as reference compounds was dissolved like the other compounds.

Cell lines, cell culture and cell growth assay. The human papillary thyroid carcinoma (PTC) cell lines TPC-1 and Nim-1 were grown in Dulbecco's modified Eagle's medium (DMEM) (Lonza, Verviers, Belgium) supplemented with 10% fetal bovine serum whereas the K1 cell line was cultured in DMEM: Ham's F12 (Lonza): MCDB 105 (Sigma) (2: 1: 1) supplemented with 20% serum. The ovarian carcinoma cell line IGROV-1 [41] was routinely maintained in RPMI medium (Lonza) containing 10% serum. All cell lines were incubated at 37 °C in 5% CO₂ atmosphere. TPC-1 cells harbor the RET/PTC-1 rearrangement, Nim-1 cells the BRAFV600E mutation, and K1 cells both BRAF V600E and PI3K E542K mutation [42]. Down-regulation of PTEN has been described in Nim-1 cells [35]. IGROV-1 cells harbor hetT319F deletion and frameshift in PTEN, hetR38C mutation in the p85 binding domain of p110 α and an additional hetX1069W mutation that extends the C-terminus of p110 α by four amino acids [36]. For cell growth assay, cells were plated in 12 well-plates at 5000 cells/cm² (Nim-1), 3000 cells/cm² (TPC-1), or 4000 cells/cm² (K1), in complete medium. One day after seeding, cells were exposed to solvent (DMSO, 0.5% final concentration) or to increasing drug concentrations for 72h. IGROV-1 cells were plated in complete medium (at 5000 cells/cm²). The day after, cells were serum starved and treated with the drugs for 24h. The supernatant was then removed and complete medium was added for further 48 h. Next, cells were trypsinized and counted by a Coulter Counter (Coulter Electronics, Luton, UK). Each experiment was performed in

duplicates. The percentages of survival in drug-treated *versus* untreated samples are reported in dose-response curves. IC_{50} represent drug concentrations able to inhibit cell proliferation by 50%. Statistical analyses were performed using Student's 2-tailed t test. A value of $p < 0.05$ was considered statistically significant.

Western blot analysis. IGROV-1 cells were seeded in complete medium and, 24 h later, serum starved and treated with the indicated concentrations of the drugs. After 24 h, cells were processed for total protein extraction and immunoblot analysis was performed as previously described [43]. The following rabbit polyclonal antibodies were used: anti-phospho-GSK-3 α β (Ser21/9) from Cell signaling (Beverly, MA), anti-GSK-3 β and anti-phospho-BAD (Ser136) from Santa Cruz Biotechnology (Santa Cruz, CA) and anti-actin (Sigma). A mouse monoclonal antibody against BAD was obtained from Transduction Laboratories (Lexington, KY). Immunoreactive bands were revealed by enhanced chemiluminescence detection system ECL (GE Healthcare, UK). Band intensities were quantified by ImageJ developed by Wayne S. Rasband (National Institutes of Health, Bethesda, Maryland).

Acknowledgments

We gratefully acknowledge Fondazione CARIPLO under project 2011-0490 "Targeting pro-survival features of tumor cells by novel inhibitors of the Akt kinase", "Fondo Per La Promozione di Accordi Istituzionali"–Regione Lombardia, under project NEDD (Network Enabled Drug Design) 14546/2010, and Associazione Italiana per la Ricerca sul Cancro (IG15333 to PP) for financial support. The authors thank also Laura Dal Bo, Nives Carenini, Enrica Favini for technical support, Mr Andrea Lorenzi for MS technical support and Prof. Fiamma Ronchetti for helpful discussion.

References

1. Jänne, P. A.; Gray, N.; Settleman, J. *Nat. Rev. Drug Discov.* **2009**, 8, 709.
2. Levitzki, A.; Mishani, E. *Ann. Rev. Biochem.* **2006**, 75, 93.
3. Levitzki, A. *Acc. Chem. Res.* **2003**, 36, 462.
4. Fruman, D.; Rommel, C. *Nat. Rev. Drug Discov.* **2014**, 13, 140.
5. Cohen, P. *Nat. Chem. Drug Discov.* **2002**, 1, 309.
6. Kohn, M. *Bioorg. Med. Chem.* **2015**, 23, 2747.
7. Lapenna, S.; Giordano, A. *Nat. Rev. Drug Discov.* **2009**, 8, 547.
8. Cassinelli, G.; Zuco, V.; Gatti, L.; Lanzi, C.; Zaffaroni, N.; Colombo, D.; Perego, P. *Curr. Med. Chem.* **2013**, 20, 1923.
9. Mabuchi, S.; Kuroda, H.; Takahashi, R.; Sasano, T. *Gynecol. Oncol.* **2015**, 137, 173.
10. Vanhaesebroeck, B.; Stephens, L.; Hawkins, P. *Nat. Rev. Mol. Cell Biol.* **2012**, 13, 195.
11. Meuillet, E. J. *Curr. Med. Chem.* **2011**, 18, 2727.
12. Granville, C. A.; Memmott, R. M.; Gills, J.; Dennis, P. A. *Clin. Cancer Res.* **2006**, 12, 679.
13. Toker, A.; Yoeli-Lerner, M. *Cancer Res.* **2006**, 66, 3963.
14. Radaelli, C.; Granucci, F.; De Gioia, L.; Cipolla, L. *Mini Rev. Med. Chem.* **2006**, 6, 1127.
15. Maffucci, T.; Falasca, M. *FEBS Lett.* **2001**, 506, 173.
16. Rong, S. B.; Hu, Y.; Enyedy, I.; Powis, G.; Meuillet, E. J.; Wu, X.; Wang, R.; Wang, S.; Kozikowski, A. P. *J. Med. Chem.* 2001, 44, 898.
17. Calleja, V.; Laguerre, M.; Parker, P. J.; Larijani, B. *PLOS Biol.* **2009**, 7, e17.
18. Scheid, M. P.; Woodgett, J. R. *FEBS Lett.* **2003**, 546, 108.

19. Cherétien, F.; Moitessiera, N.; Roussella, F.; Maugerb, J. P.; Chapleur, Y. *Curr. Org. Chem.* **2000**, 4, 513.
20. Cipolla, L.; Redaelli, C.; Granucci, F.; Zampella, G.; Zaza, A.; Chisci, R.; Nicotra, F. *Carbohydr. Res.* **2010**, 345, 1291.
21. Gabrielli, L.; Calloni, I.; Donvito, G.; Costa, B.; Arrighetti, N.; Perego, P.; Colombo, D.; Ronchetti, F.; Nicotra, F.; Cipolla, L. *Eur. J. Org. Chem.* **2014**, 5962.
22. Benson, A. A.; Daniel, H.; Wister, R. *Proc. Natl. Acad. Sci. USA.* **1959**, 45, 1582.
23. Benning, C. *Annu. Rev. Plant Physiol. Plant Mol Biol.* **1998**, 49, 53.
24. Matsuji, K.; Tanabe, A.; Hongo, A.; Sugawara, F.; Sakaguchi, K.; Takahashi, N.; Sato, N.; Sahara, H. *Cancer Sci.* **2012**, 103, 1546.
25. Dangate, M.; Franchini, L.; Ronchetti, F.; Arai, T.; Iida, A.; Tokuda, H.; Colombo, D. *Bioorg. Med. Chem.* **2009**, 17, 5968.
26. Dangate, M.; Franchini, L.; Ronchetti, F.; Arai, T.; Iida, A.; Tokuda, H.; Colombo, D. *Eur. J. Org. Chem.* **2009**, 6019.
27. Colombo, D.; Gagliardi, C.; Vetro, M.; Ronchetti, F.; Takasaki, M.; Konoshima, T.; Suzuki, N.; Tokuda, H. *Carbohydr. Res.* **2013**, 373, 64.
28. Lehmann, J.; Weckerle, W. *Carbohydr. Res.* **1975**, 42, 275.
29. Compton, J. *J. Am. Chem. Soc.* **1938**, 60, 395.
30. Vetro, M.; Costa, B.; Donvito, G.; Arrighetti, N.; Cipolla, L.; Perego, P.; Compostella, F.; Ronchetti, F.; Colombo, D. *Org. Biomol. Chem.* **2015**, 13, 1091.
31. Fensterle, J.; Aicher, B.; Seipelt, I.; Teifel, M.; Engel, J. *Anti-Cancer Agents Med. Chem.* **2014**, 14, 629.
32. Milburn, C. C.; Deak, M.; Kelly, S. M.; Price, N. C.; Alessi, D. R.; Van Aalten, D. M. F. *Biochem. J.* **2003**, 375, 531.

33. Xing, M. *Thyroid*. **2010**, 20, 697.
34. Liu, D.; Hou, P.; Liu, Z.; Wu, G.; Xing, M. *Cancer Res*. **2009**, 69, 7311.
35. Bruni, P.; Boccia, A.; Baldassarre, G.; Trapasso, F.; Santoro, M.; Chiappetta, G.; Fusco, A.; Viglietto, G. *Oncogene* **2000**, 19, 3146.
36. Raynaud, F. I.; Eccles, S. A.; Patel, S.; Alix, S.; Box, G.; Chuckowree, I.; Folkes, A.; Gowan, S.; De Haven Brandon, A.; Di Stefano, F.; Hayes, A.; Henley, A. T.; Lensun, L.; Pergl-Wilson, G.; Robson, A.; Saghir, N.; Zhyvoloup, A.; McDonald, E.; Sheldrake, P.; Shuttleworth, S.; Valenti, M.; Wan, N. C.; Clarke, P. A.; Workman, P. *Mol. Cancer Ther.* **2009**, 8, 1725.
37. Hers I.; Vincent, E. E.; Tavarè, J. M. *Cell Signal*. **2011**, 23, 1515.
38. Pettersen, E. F.; Goddard, T. H.; Huang, C. C.; Couch, G. S.; Greenblatt, D. M.; Meng, E. C.; Ferrin, T. E. *J. Comput. Chem.* **2004**, 25, 1605.
39. Lang, P. T.; Brozell, S. R.; Mukherjee, S. *RNA*, **2009**, 15, 1219.
40. Yamamoto, F.; Perucho, M. *Nucleic Acids Res.* **1984**, 12, 8873.
41. Perego, P.; Romanelli, S.; Carenini, N.; Magnani, I.; Leone, R.; Bonetti, A.; Paolicchi, A.; Zunino, F. *Ann. Oncol.* **1998**, 9, 423.
42. Schweppe, R. E.; Klopper, J. P.; Korch, C.; Pugazhenti, U.; Benezra, M.; Knauf, J. A.; Fagin, J. A.; Marlow, L.; Copland, J. A.; Smallridge, R. C.; Haugen, B. R. *J. Clin. Endocrinol. Metab.* **2008**, 93, 4331.
43. Benedetti, V.; Perego, P.; Beretta, G. L.; Corna, E.; Tinelli, S.; Righetti, S.; Leone, R.; Apostoli, P.; Lanzi, C.; Zunino, F. *Mol. Cancer Ther.* **2008**, 7, 679.

Legends to figures

Figure 1. Structure of the compounds. Structure of D-glucopyranose-based glycoconjugates targeting Akt PH domain.

Figure 2. Evaluation of Akt inhibition in cell-free assays. Inhibitory activity of compounds **2-8** against Akt. Akt activity was assayed through a specific ELISA test. Compounds were added at a concentration of 100 μ M and the data represent the mean (\pm SD) of three independent experiments. * $p < 0.05$, ** $p < 0.01$ versus vehicle (Kruskal-Wallis non parametric ANOVA).

Figure 3 Evaluation of Akt inhibition in cell-free assays as a function of compound concentration. Concentration-response (% inhibition) analysis of compound **3a**.

Figure 4. Evaluation of BTK activity in cell-free assays. Effect of compound **3a** against BTK. BTK activity was assayed through a luminescent kinase assay. Compound was tested at a concentration of 100 μ M and the data represent the mean (\pm SD) of two independent experiments. As reference compound, the Akt1/2 kinase inhibitor A6730 was used. Staurosporine was employed as positive control as indicated in the assay protocol.

Figure 5. Docking studies. Docked conformations: A, 4IP (inositol-(1,3,4,5)-tetrakisphosphate); B, compound **2a**; C, compound **2b**; D; compound **2c**; E, compound **3a**; F, compound **3b**; G, compound **3c**; H, compound **4**; I, compound **5**; J, compound **6**; K, compound **7**; L, compound **8**.

Figure 6. Focus on the orientation of the functional group SO_3^- . For every compound only group SO_3^- and the monosaccharide cycle are shown.

Figure 7. Western blot analysis of the effect of selected sulfoglycolipids on NIH 3T3 K-RAS cells. The ability of the different compounds (Cpd, 100 μM) or of the known inhibitor (A6730) to inhibit serum-induced Akt phosphorylation in NIH 3T3 K-RAS cells is shown. Control (CTR) refers to vehicle-treated cells. Analyses were performed on starved cells (0.5% NBCS), on cells pre-treated with the compound for 1 hour and on cells stimulated with serum (10% NBCS) for 30 minutes. The levels of phosphorylated Akt (P-Akt) and Akt were revealed using antibodies conjugated to horseradish peroxidase. Actin was used as loading control. A representative blot is shown in panel A. Panel B shows the densitometric analysis of the blots performed in three independent experiments. ** $p < 0.01$ versus control (Student's t test).

Figure 8. Effect of selected sulfoglycolipids on papillary thyroid carcinoma and ovarian carcinoma cell proliferation. Cells were exposed to vehicle or to different concentrations of the indicated compounds in complete medium for 72 h (A) or for 24 h (B). Cells were counted by a Coulter counter 72 h after the beginning of the treatment. Mean (\pm SEM) dose-curves from data obtained in two independent experiments are reported. * $p < 0.05$; ** $p < 0.001$; *** $p < 0.0001$ versus vehicle-treated cells. C) Inhibition of GSK-3 α , GSK-3 β and BAD phosphorylation in IGROV-1 cells exposed to compound **3a** and to the known inhibitor (A6730) as reference compound. Cells were exposed to vehicle (-) or the indicated drug concentrations for 24 h. Whole cell lysates were analyzed by Western blotting. One

representative experiment out of two is shown. Not pertinent bands were cut. Histograms refer to the quantification of band intensities normalized with respect to the actin loading control.

ACCEPTED MANUSCRIPT

